# Controls on shelf-margin architecture and sediment partitioning in the Hammerhead shelf margin (Bight Basin, southern Australia): Quantitative 3D seismic stratigraphy (QSS)

**John Shepherd**
*University of Western Australia*
john.shepherd@research.uwa.edu.au

**Simon Lang**
*University of Western Australia*
simon.lang@uwa.edu.au

**Victorien Paumard**
*University of Western Australia*
victorien.paumard@uwa.edu.au

**Annette D. George**
*University of Western Australia*
annette.george@uwa.edu.au

**Daniel Peyrot**
*University of Western Australia*
daniel.peyrot@uwa.edu.au

## SUMMARY

Understanding the stratigraphic architecture of shelf-margin clinoforms is key to determining how sediments are transported to deep-water settings and how the interplay of tectonics (subsidence/uplift) and eustasy, with variation in sediment supply, impacts deep-water sand delivery. Within this study clinothems are used to establish quantitative and statistical relationships between the shelf-margin architecture, paleoshoreline processes, and deep-water system types (i.e., using quantitative 3D seismic stratigraphy). In the Bight Basin on the southern margin of Australia, the Hammerhead shelf margin prograded during the Late Cretaceous following continental rifting from Antarctica. This understudied interval offers an opportunity to investigate controls on shelf-margin evolution during the early post-rift phase. All available data (2D seismic data, 3D seismic data and well data) from the Ceduna Sub-basin have been integrated to investigate the controls on shelf-margin architecture and factors affecting sediment delivery to deep water. Quantitative analyses of clinoform geometry are used to calculate several parameters at 3$^{rd}$ order and 4$^{th}$–5$^{th}$ order scales. Sixteen 3$^{rd}$ order seismic sequences and 28 4$^{th}$–5$^{th}$ order clinothems with an average duration of ~ 67 kyrs are recognised. Four phases of Hammerhead shelf-margin evolution are identified with lateral variations in sediment supply proposed to be the main driver of shelf-margin variability. We propose that after a major flooding event, the A/S ratio increased throughout the evolution of the Hammerhead with an increase in accommodation and a rapid decline in sediment supply in the Maastrichtian causing backstepping of the shelf edge. At higher resolution, results show shelf-margin architecture, shoreline processes, and deep-water system types are intimately linked. For example, wave-dominated shorelines are related to no (or very little) deep-water deposition whereas fluvial-dominated shorelines are mostly linked with MTD's and/or long runout turbidite systems. Results of this research may be applied to other basins developed in similar tectonic and climatic settings.

**Key words:** Hammerhead shelf margin, Bight Basin, Sediment supply, Accommodation, Sediment partitioning

## INTRODUCTION

Clinoforms are inclined, commonly basinward-dipping, chronostratigraphic stratal surfaces that represent the dominant architectural component of source-to-sink systems (e.g., Patruno et al., 2015; Pellegrini et al., 2020). To understand the distribution of reservoir sands in deep-water areas of basins, a sound knowledge of processes operating in shallower areas is needed (e.g., the entire source-to-sink system; Helland-Hansen et al., 2016). Shelf margins represent a crucial point along the source-to-sink system where sediments are partitioned from the shelf to slope and basin-floor areas (Helland-Hansen et al., 2016). The spatial and temporal arrangement of shelf-margin clinothems record past accommodation and sediment supply settings as well as showing how sediments have been transported to deep-water areas within a basin (Gong et al., 2016a). Historically, sand delivery to deep water was considered a function of only two parameters namely accommodation, and sediment supply (Vail et al., 1977). Recent studies, however, are demonstrating that the delivery of reservoir-quality sand to slope and basin-floor areas is more complex with factors now proposed to modulate this sand delivery including accommodation, sediment supply, grain size, shoreline processes, shelf width, slope gradient, shelf-basin relief, tectonic regime, and climate (Carvajal et al., 2009; Gong et al., 2016a, 2016b; Paumard et al., 2020, 2019b).

The Bight Basin (Figure 1) has a complex tectono-stratigraphic evolution with several episodes of extension and thermal subsidence leading up to the final break-up of Antarctica and Australia in the Santonian (Kempton et al., 2020;

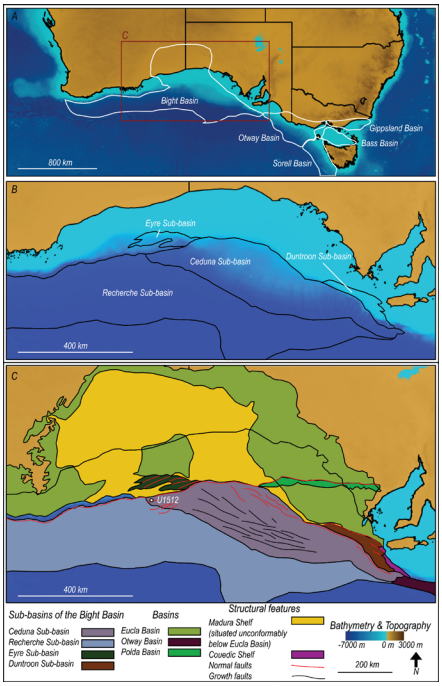


**Figure 1. (a) Location map of the major basins (outlined in white) along Australia's southern margin. State and territory boundaries of southern Australia shown in black. (b) Map showing sub-basins of the Bight Basin although the Bremer Sub-basin is located to the west of this map. (c) More detailed map of sub-basins and major tectonic elements of the southern margin of Australia (after Bradshaw, 2003). Location of IODP Site U1512 is also shown. Topographic (metres above modern sea level) and bathymetric (metres below modern sea level) data from the Geoscience Australia database (Whiteway, 2009).**

Krassay and Totterdell, 2003; Totterdell et al., 2000). Following break-up, a combination of high sediment supply from the hinterland and high subsidence rates in the Bight Basin promoted continuous progradation of the thick and extensive Hammerhead shelf margin (Krassay and Totterdell, 2003; MacDonald et al., 2013; Totterdell et al., 2000). Shelf-margin clinoforms record specific physiographic and environmental conditions (e.g., sea level, climate, sediment supply and accommodation; Gong et al., 2015) so the Hammerhead shelf margin records the early stages of separation of Australia and Antarctica. However, previous regional stratigraphic studies have been limited by a lack of data coverage and resolution, and made more complicated by the presence of extensive gravity-driven growth faulting affecting this interval (Totterdell et al., 2000). Typically, these studies relied on sparse regional 2D seismic data integrated with rare available well data (e.g., Totterdell et al., 2000). The stratigraphic framework presented by Totterdell et al. (2000) focussed on the 2nd order, i.e., 'supersequence' scale with only minor revisions throughout the last two decades (e.g., (Kempton et al., 2020; Krassay and Totterdell, 2003).

By using high-resolution 3D seismic data (i.e., Ceduna 3D seismic survey) and full-volume seismic interpretation software (i.e., Paleoscan™) we employ a dynamic stratigraphic approach (Henriksen et al., 2011) to the Hammerhead shelf margin, to: 1) quantitatively characterise the architecture and development (e.g., clinoform slope gradient, shelf-edge trajectory, progradation rate etc.) of 16 key 3$^{rd}$ order seismic sequences that comprise the Hammerhead shelf margin in order to refine the stratigraphic framework and investigate controls on shelf margin architecture; 2) quantitatively investigate, at higher resolution, 28 4$^{th}$/5$^{th}$ order paleo-shelf margins which focus on the lower and lowermost middle Hammerhead; 3) apply the shallow marine process-based classification scheme of Ainsworth et al. (2011) to paleoshorelines from these 28 high-resolution shelf margins; and 4) analyse the presence of coeval deep-water deposits. Using this approach, referred to by (Paumard et al., 2019a) as quantitative seismic stratigraphy, allows for investigation of the relationships between shallow marine processes, stratigraphic architecture, and deep-water sediment delivery in the Hammerhead shelf margin. Understanding these relationships is key for improving the predictability of potential reservoir deposits in shallow- and deep-water areas of basins.

## DATASETS AND METHODS

### Datasets

The open-file Ceduna 3D seismic dataset was used for all 3D seismic interpretations in this study (Figure 2). This seismic survey covers an area of 12,022 km$^2$, with a bin size of 12.5 m x 30 m and a 2 ms sampling rate. The Flinders Deepwater 2D seismic survey was used to tie-in biostratigraphic data from wells outside the Ceduna 3D seismic area, and to regionally map four key surfaces from the Hammerhead Supersequence (Figure 3). This 2D seismic survey comprises 117 lines with a total line length of 15 636 km, with a 2 ms sampling rate. Well logs and biostratigraphic data from three wells have been used: Gnarlyknots-1A; Potoroo-1; and Greenly-1. These wells provide lithostratigraphic, biostratigraphic and stratigraphic control on seismic interpretations (Figure 2; Table 1).

### Methods

Using the seismic stratigraphic methods of Mitchum et al. (1977) and geometric attributes which highlight surfaces where reflectors either diverge or converge, 17 regional seismic unconformities (e.g., surfaces of downlap, toplap, and/or onlap) were identified in the Hammerhead shelf margin (Figure 3). These surfaces were calibrated with biostratigraphic data from the Gnarlyknots-1A well using the Flinders Deepwater 2D seismic survey. The low resolution of the 2D seismic data prevents refined biostratigraphic calibration but enables us to date/use four major key surfaces identified within the Hammerhead shelf margin (Figure 3; Table 1). As such, duration of the 3$^{rd}$ order seismic sequences identified in this study are estimated based on the duration of, and number of sequences within, each of the three major intervals. Paleoscan™ was used for full-volume 3D seismic interpretation. The standard workflow in Paleoscan™ is an iterative process and comprises three main steps, model-grid computation, RGT model (3D

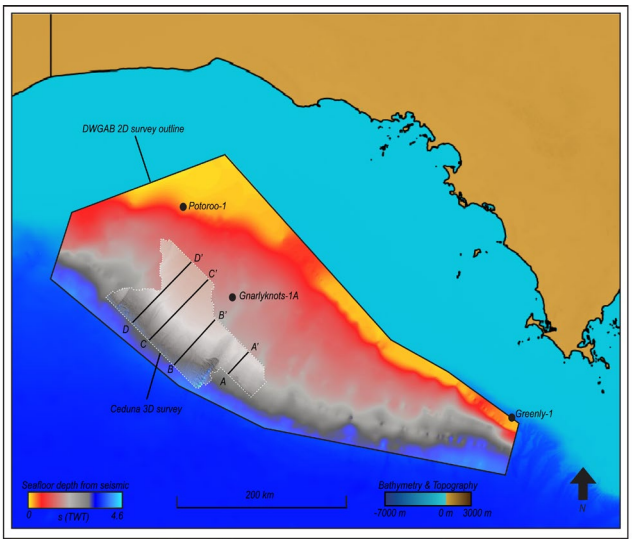


**Figure 2. Location of the datasets used in this study. Background bathymetry data from Geoscience Australia (Whiteway, 2009), overlying higher resolution seafloor depth (s TWT) data is from Flinders Deep Water (DWGAB) 2D Seismic Survey (black outline) and Ceduna 3D seismic survey (white dashed outline). Location of key wells (black circles): Potoroo-1; Gnarlyknots-1A; and Greenly-1. A–A' represents seismic crossline 5000 (SE Ceduna), B–B' represents seismic crossline 9250 (Central Ceduna), C–C' represents seismic crossline 11725 (Central Ceduna), and D–D' represents seismic crossline 13500 (NW Ceduna) from the Ceduna 3D seismic survey.**

geomodel) calculation, and horizon stack extraction. Velocity data from Gnarlyknots-1A were used to determine approximate depths of the four major key seismic unconformities. Interval velocities from Gnarlyknots-1A within the Hammerhead Supersequence suggest an average velocity of 3000 m/s, and this velocity was used to convert geometric measures from two-way-time (TWT) to depth.

Quantitative analysis at both 3rd and 4th/5th order involved measurement of shelf margin geometries of individual seismic sequences on four dip-oriented seismic lines (e.g., Figure 3). Several measurements were taken, including: sequence sediment thickness; topset sediment thickness; bottomset sediment thickness; clinoform height; clinoform slope gradient; relative shelf margin aggradation; and relative shelf margin aggradation.

From these measurements several parameters were calculated, including: shelf-edge trajectory angle ($T_{se}$), progradation rate ($R_p$), aggradation rate ($R_a$), topset sedimentation rate ($A_t$), bottomset sedimentation rate ($A_b$), topset/bottomset aggradation ratio ($A_t/A_b$), and progradation/aggradation ratio ($P_{se}/A_{se}$).

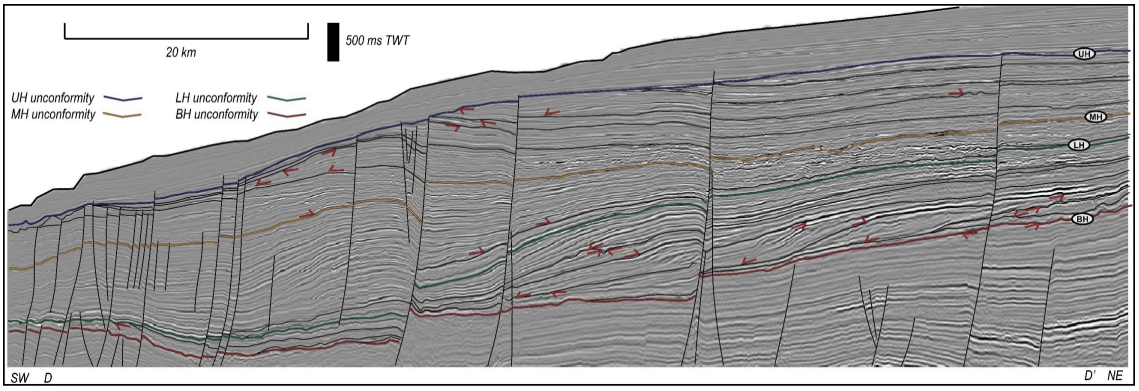


**Figure 3. Interpreted seismic crossline 13500 from the Ceduna 3D dataset (see Figure 2 for location; D–D'). Interpretation includes tectonic structures, key surfaces, and reflection terminations. Note the flatter shelf-edge trajectories below the LH unconformity.**

From this quantitative analysis, 6 main types of shelf margin architecture are identified: 1) falling ($T_{se} < 0^o$, $P_{se}/A_{se} < 0$, progradational stacking pattern), 2) flat ($0^o < T_{se} < 0.5^o$, $P_{se}/A_{se} > 115$, progradational stacking pattern), 3) slightly rising ($0.5^o < T_{se} < 1^o$, $115 > P_{se}/A_{se} > 55$, progradational and slightly aggradational stacking pattern), 4) moderately rising ($1^o < T_{se} < 2^o$, $55 > P_{se}/A_{se} > 28$, progradational and aggradational stacking pattern), 5) steeply rising ($T_{se} > 2^o$, $P_{se}/A_{se} < 28$, progradational and strongly aggradational stacking pattern), and 6) backstepping ($T_{se} < 0^o$, $P_{se}/A_{se} < 0$, retrogradational stacking pattern).

Paleoshorelines from the lower and lowermost middle Hammerhead have been classified using the process-based, shallow marine (WAVE) classification outlined by Ainsworth et al. (2011). This classification scheme is based on the relative importance of primary, secondary, and tertiary processes operating in shoreline depositional environments (Ainsworth et al., 2011). To classify a paleoshoreline, depositional elements observed along a stretch of coastline (e.g., mouth bars, distributary channels, incised valleys, and beach ridges) are linked to paralic processes (e.g., fluvial, wave, and tidal). Within this interval four types of deep-water systems are recognised, areas with no visible deep-water deposition are also noted. The deep-water systems investigated in this study are sheet sands (Type 1), mass-transport deposits (MTDs; Type 2), short run-out turbidite systems (Type 3), and long run-out turbidite systems (Type 4).

**Table 1. Regional key surfaces from the Hammerhead shelf margin. Key surfaces picked using Ceduna 3D seismic survey with tie-lines to Gnarlyknots-1A from Flinders Deepwater 2D seismic survey. Age calculation largely based on palynology report of Gnarlyknots-1A by Morgan (2014).**

| Surface | TWT (ms) | MD | Age |
|---|---|---|---|
| UH | 2090 | 1998 | End Maastrichtian. Based on palynology data from Potoroo 1, correlated to regional 2D seismic survey. No palynology completed from Gnarlyknots-1A – still very high numbers of *F. longus* at 2150/60 MD (e.g. still in *F. longus* (Upper) Spore-Pollen Zone). |
| MH | 2655 | 2530 | At base of *F. longus* (Lower) Spore Pollen Zone and no dinoflagellate zone attributed – late Campanian |
| LH | 3040 | 2895 | *N. senectus* (Middle) Spore-Pollen Zone – early Campanian |
| BH | 3855 | 3738 | *T. apoxyexinus* (Upper) Spore-Pollen Zone and *I. cretaceum* Dinoflagellate Zone – middle to late Santonian |

## RESULTS AND DISCUSSION

### 3rd order shelf-margin evolution and controls on architecture

The Hammerhead interval can be divided into three major intervals (e.g., Krassay and Totterdell, 2003), herein named the lower Hammerhead, middle Hammerhead, and upper Hammerhead (Figures 3, 4). These intervals are bounded by four major key surfaces, namely the Base Hammerhead (BH) unconformity, Lower Hammerhead (LH) unconformity, Middle Hammerhead (MH) unconformity, and Upper Hammerhead (UH) unconformity (Figure 3). Biostratigraphic ages of these key surfaces are presented in Table 1.

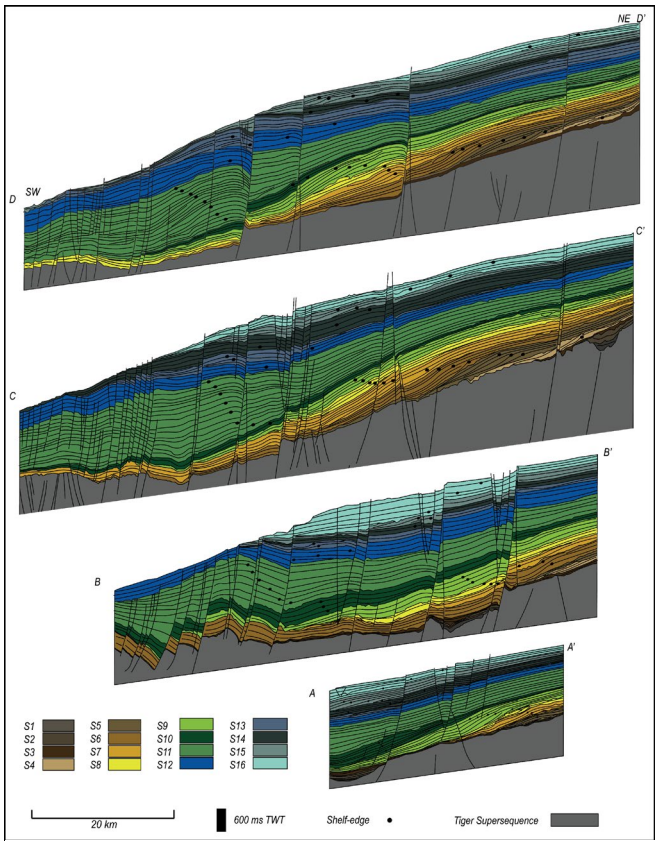


**Figure 4. Internal geometries of seismic sequences within the Hammerhead shelf-margin. From seismic crosslines: A–A'; B–B'; C–C'; and D–D'. See Fig. 8 for crossline location. Black circles represent the location of the shelf-edge. Significant lateral and vertical variability is demonstrated by thickness differences between sequences and within a sequence laterally along the shelf margin.**

Stratigraphic architecture of the Hammerhead shelf margin is observed to be highly variable both laterally (along the shelf edge) and vertically (Figure 4). The mid Santonian to lower Campanian lower Hammerhead comprises the most complete record of clinoforms within the Ceduna Sub-basin. Nine seismic sequences (S1 to S9) are identified within the lower Hammerhead and S1–S3 appear in seismic as parallel, canyon-filling reflectors whereas S4–S9 are progradational clinoforms with oblique tangential geometries (Figure 4). Stratal stacking patterns are more aggradational in the Campanian middle Hammerhead, and two seismic sequences are identified (S10–S11; Figure 4). The clinoforms of both S10 and S11 display oblique tangential geometry (Figure 4). The upper Campanian–Maastrichtian upper Hammerhead (S12–S16) displays predominantly retrogradational stratal stacking patterns in contrast to the lower and middle Hammerhead progradational and aggradational patterns respectively (Figure 4). Five seismic sequences are identified (Figure 4). Oblique tangential clinoform geometry with a progradational stacking pattern is observed in S13 and S15, and retrogradational stratal stacking patterns are observed in S12, S14, and S16 (Figure 4).

Changes in shelf-margin architecture (e.g., shelf-edge trajectories, stratal stacking patterns, and sediment thickness) though time are used to interpret the stratigraphic evolution of the Hammerhead interval. This study proposes that the

Hammerhead interval evolved through four distinct phases: Phase 1 (lower Hammerhead canyon fill) characterised by local deposition of marine mudstones interpreted to record an initial major flooding event in the Ceduna Sub-basin; Phase 2 (lower Hammerhead post-canyon fill) marking the onset of progradation within the Hammerhead interval with overall shelf-margin growth characterised by slightly to moderately rising shelf-edge trajectories (A/S<<1) in the northwest and central parts of the Ceduna Sub-basin, and moderately rising to steeply rising shelf-edge trajectories in the southeast (A/S<1) as a supply-dominated shelf margin (*sensu* Gong et al., 2016a, 2015a, 2015b); Phase 3 (middle Hammerhead) with continued progradation of the shelf margin and shelf-edge trajectories that are steeper than those of Phase 2, with shelf-margin growth dominated by steeply rising shelf-edge trajectories (A/S=1) and a shelf margin that can no longer be classified as supply dominated; and Phase 4 (upper Hammerhead) which represents a change in depositional characteristics with overall retrogradation signifying significantly reduced sediment supply alongside increased accommodation creation (A/S>>1) interrupted by two brief periods of progradation.

Several factors can affect shelf-margin architecture including sediment loading and lithospheric cooling, eustasy and climate, and sediment supply. The relative impacts of these factors for the Hammerhead shelf margin have been investigated, and whereas sediment loading and lithospheric cooling (i.e., thermal subsidence) was the major control on accommodation creation at 1st order post break-up, shelf-margin variability between the 3rd order sequences suggest other factors were also important. For example, the major factor controlling the lateral variability present in the Hammerhead shelf margin is interpreted to be changes, both laterally and through time, in sediment supply.

**High-resolution investigation: shoreline processes and deep-water deposits**

To extract the maximum resolution from the Ceduna 3D dataset a high-resolution seismic interpretation workflow was applied to the lower and lowermost middle Hammerhead. 28 seismic sequences (i.e., clinothems; Figure 5) were identified, and 20 of these (C1–C20) comprise the lower Hammerhead (above the basal incised valley/canyon system) and biostratigraphic data constrain the duration of this interval to ~ 1.3 Myrs, and the clinothems identified in this interval have an estimated duration of ~ 67,000 yrs each (e.g., 5th stratigraphic order; *sensu* Vail et al., 1991). This estimated duration has also been applied to the eight clinothems that are situated in the lowermost middle Hammerhead (C21–C28; Figure 5).

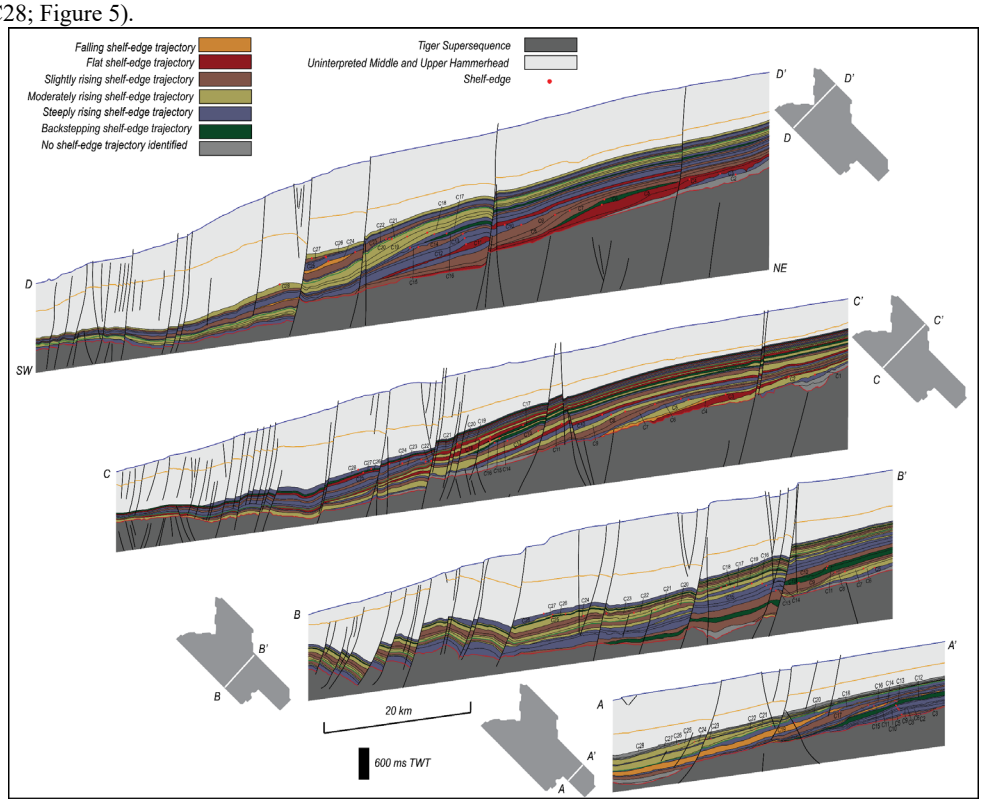


**Figure 5. geometries of seismic sequences within the Hammerhead shelf-margin, with sequences coloured based on shelf-edge trajectory angle. From seismic lines: A–A'; B–B'; C–C'; and D–D'. See Figure 2 for line location.**

The classification of paleoshorelines is based on the identification of two main elements in seismic geomorphology, corresponding to areas of interpreted wave (i.e., beach ridges and beach ridge sets) and fluvial (i.e., channels) dominance respectively. In areas where both features are identified, analysis of the varying proportions of these elements has been used to distinguish between the mixed-process shorelines of Ainsworth et al., (2011). Based on seismic geomorphological analysis and cross-sectional 3D architecture, five paleoshoreline types have been identified

in the 28 high resolution seismic sequences: wave-dominated (W); wave-dominated, fluvial-influenced, and tide-affected (Wf*t*); fluvial-dominated, wave-influenced, and tide-affected (Fw*t*); fluvial-dominated, tide-influenced, and wave-affected (Ft*w*); and fluvial-dominated and tide-influenced (Ft).

Four types of deep-water systems are identified and areas with no visible deep-water deposition are also noted. Sheet sands (Type 1), mass-transport deposits (MTDs; Type 2), short run-out turbidite systems (Type 3), and long run-out turbidite systems (Type 4) are all observed within C1–C28.

Sediment partitioning to deep-water settings can be significantly affected by shelf-margin architecture and shoreline processes (Gong et al., 2016a, 2016b; Paumard et al., 2020, 2019b). Therefore, lateral variations in this architecture and changes to shoreline processes along the shelf edge will have a major impact on how sediments are transported to deep water. (Gong et al., 2015a) demonstrated an effective first-order method for analysing sediment partitioning, and this involves comparing shelf-edge trajectory angles ($T_{se}$) with differential sedimentation ratios between topsets and bottomsets ($A_t/A_b$; Figure 6).

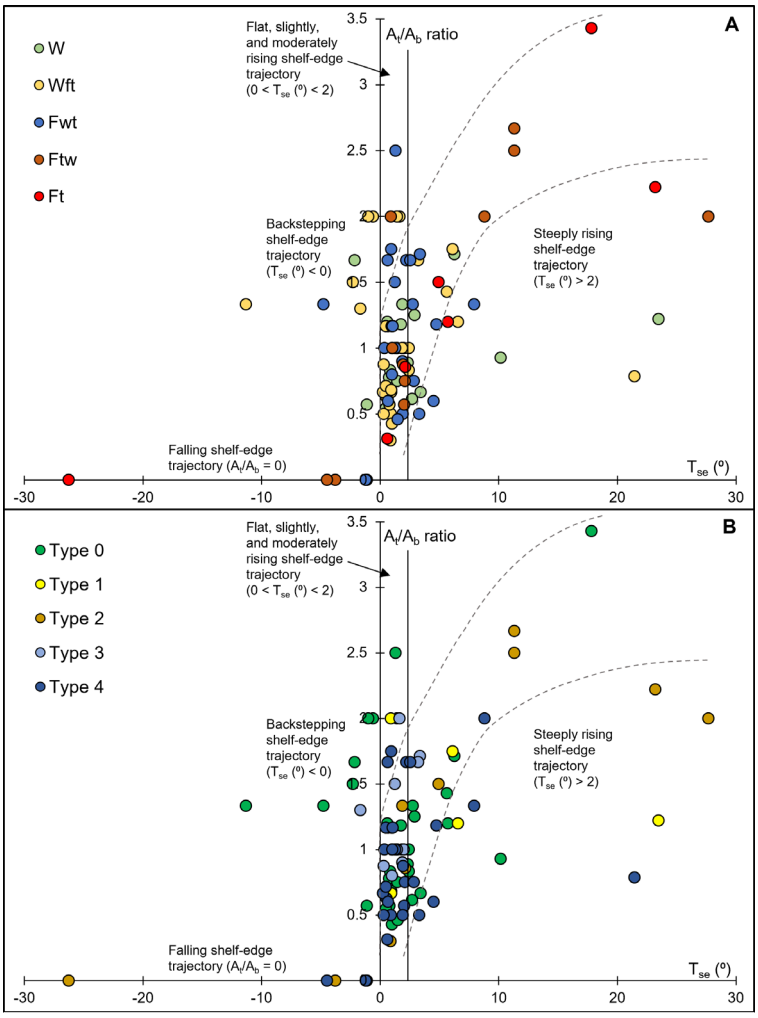


**Figure 6. Differential sedimentation between topsets and bottomsets ($A_t/A_b$) plotted against shelf-edge trajectory angle ($T_{se}$) for each clinothem (C1–C28) identified. A) Datapoints sorted by shoreline classification (*sensu* Ainsworth et al., 2011). B) Datapoints sorted by deep-water system type.**

Clinothems with falling shelf-edge trajectories ($T_{se}$ < 0º) are always related to $A_t/A_b$ ratios of 0 (Figure 6). This means that all sediments are bypassing the shelf and being deposited in deep-water areas (i.e., thicker bottomsets). Interestingly, all clinothems in this category are linked to fluvial-dominated shorelines (Fw*t*, Ft*w*, or Ft; Figure 6a) and either MTD's (Type 2) or long runout turbidite systems (Type 4) in deep-water settings (Figure 6b). Alternately, backstepping shelf-edge trajectories ($T_{se}$ < 0º) are mostly associated with $A_t/A_b$ ratios of 1–2 (Figure 6). This suggests that little sediment is reaching deep-water areas and that much more sediment is being stored on the shelf (i.e., thicker topsets). Almost all clinothems with backstepping shelf-edge trajectories are associated with no deep-water depositional features (Type 0; Figure 6b), and wave-dominated shorelines (e.g., W or Wf*t*; Figure 6a). $A_t/A_b$ ratios of 0–1 are commonly linked to clinothems with flat, slightly and steeply rising shelf-edge trajectories (0º < $T_{se}$ < 2º; Figure 6), however, some of these clinothems display $A_t/A_b$ ratios of up to 2.5 (Figure 6). For most clinothems in this category more sediment is delivered to deep-water areas than is stored on the shelf (i.e., thicker bottomsets). All types of shorelines and deep-water systems are observed within clinothems in this category (Figure 6). Clinothems that have steeply rising shelf-edge trajectories ($T_{se}$ > 2º) are mostly associated with $A_t/A_b$ ratios of 1–3.5 (Figure 6), and while there are several examples of lower $A_t/A_b$ ratios (i.e., 0.5–1; Figure 6), these mainly occur within clinothems of this category with gentler shelf-edge trajectories (i.e., 2º < $T_{se}$ < 4º; Figure 6). Most sediments in clinoforms of this category are stored on the shelf (i.e., thicker topsets). The majority of measurements in this category fall within an expected range that broadly correlates to increasing $T_{se}$'s being associated with increasing $A_t/A_b$ ratios (Figure 6). Measurements that fall outside of this range all have $A_t/A_b$ ratios lower than expected (Figure 6) and this is likely due to lateral supply of sediment or slope failure. All shoreline types and deep-water systems are represented in this category (Figure 6).

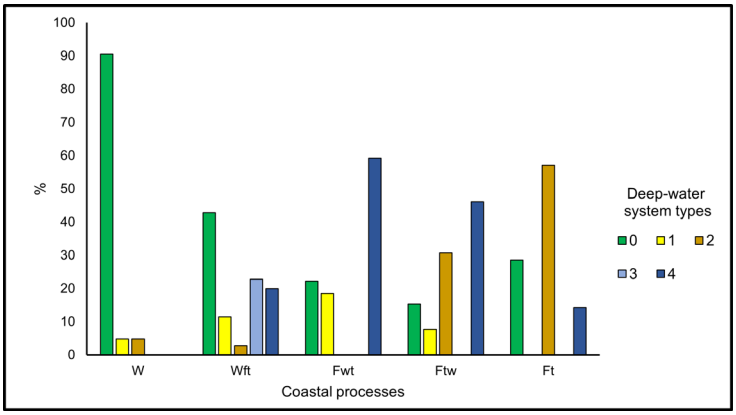


**Figure 7. Relative proportion of deep-water systems present for each type of shoreline process identified. Shoreline processes transition from more wave-dominated to the left to more fluvial-dominated to the right, note the increase in Type 2 (MTD's) and Type 4 (Long runout turbidite systems) deep-water deposits as more fluvial input is observed.**

As expected, areas of no deep-water depositional systems dominate directly offshore from wave-dominated coastlines with no fluvial influence (Figure 7). As fluvial influence increases from Wf*t* to Fw*t* long run-out turbidite systems become the dominant deep-water depositional style. However, as fluvial dominance continues but wave-influence decreases (i.e., Fw*t* to Ft*w* to Ft) the proportion of long run-out turbidite systems decreases and MTD's become the dominant style of deep-water deposition (Figure 7). We suggest that this increase in MTD's offshore from Ft*w* and Ft shorelines is due to the increased clinoform slope gradient associated with these shorelines, thus increasing the likelihood of slope failure.

## CONCLUSIONS

This study integrated regional 3D (Ceduna 3D) and 2D (Flinders Deepwater) seismic data interpretation with biostratigraphic data (Gnarlyknots-1A and Potoroo-1) to revise the 3rd order stratigraphic framework for the Hammerhead shelf margin of the Ceduna Sub-basin. This framework is used to re-interpret evolution of the Hammerhead shelf margin via four discrete phases. In this interpretation, following canyon formation and a major flooding event (Phase 1), the A/S ratio increased throughout the evolution of the Hammerhead shelf margin (Phase 2 and 3) with increasing accommodation creation and an abrupt reduction in sediment supply in the Maastrichtian causing backstepping of the shelf edge (Phase 4). At this 3rd order scale, significant lateral and vertical variability is present (particularly in the lower Hammerhead) and it is suggested that the potential driver of this variability was lateral variations in sediment supply.

High-resolution quantitative seismic interpretation with seismic geomorphology has been used to show the linkages between shelf-margin architecture, shoreline processes, and deep-water system types. Clinothems with backstepping and steeply rising shelf-edge trajectories typically have high $A_f/A_b$ ratios (i.e., > 1) meaning that more sediment is stored on the shelf. In contrast, clinothems with falling or flat, slightly, and moderately rising shelf-edge trajectories are commonly associated with $A_f/A_b$ ratios (i.e., < 1) meaning that more sediment is transferred to deep water. Results also show that wave-dominated shorelines are mostly related to no (or very little) deep-water deposition whereas fluvial-dominated shorelines are typically linked to MTD's and/or long runout turbidite systems.

## ACKNOWLEDGMENTS

We thank industry sponsors of the Quantitative Seismic Stratigraphy (QSS) Phase 2 Research Consortium (BHP, Chevron, ConocoPhillips, PGS, Santos, Shell, TGS, and Woodside) for their support and the Western Australian Department of Mines, Industry Regulation and Safety and Geoscience Australia for providing open-file 2D, 3D seismic and well data. IHS and Eliis are also thanked for providing Kingdom© and PaleoScan© software. JS acknowledges a University Postgraduate Award from the University of Western Australia, an Australian Government Research Training Program Fees Offset Scholarship, a PESA Horstman Federal Postgraduate Scholarship and additional project funding from the AAPG Grant-in-Aid Program. Additional support was received from the Centre for Energy Geoscience and the School of Earth Sciences at the University of Western Australia.

## REFERENCES

Ainsworth, R.B., Vakarelov, B.K., Nanson, R.A., 2011. Dynamic spatial and temporal prediction of changes in depositional processes on clastic shorelines: Toward improved subsurface uncertainty reduction and management. AAPG Bulletin 95, 267–297.

Bradshaw, B.E., 2003. A revised structural framework for frontier basins on the southern and southwestern Australian continental margin.

Carvajal, C., Steel, R., Petter, A., 2009. Sediment supply: The main driver of shelf-margin growth. Earth-Science Reviews 96, 221–248.

Gong, C., Steel, R.J., Wang, Y., Lin, C., Olariu, C., 2016a. Shelf-margin architecture variability and its role in sediment-budget partitioning into deep-water areas. Earth-Science Reviews 154, 72–101.

Gong, C., Steel, R.J., Wang, Y., Lin, C., Olariu, C., 2016b. Grain size and transport regime at shelf edge as fundamental controls on delivery of shelf-edge sands to deepwater. Earth-Science Reviews 157, 32–60.

Gong, C., Wang, Y., Pyles, D.R., Steel, R.J., Xu, S., Xu, Q., Li, D., 2015a. Shelf-edge trajectories and stratal stacking patterns: Their sequence-stratigraphic significance and relation to styles of deep-water sedimentation and amount of deep-water sandstone. AAPG Bulletin 99, 1211–1243.

Gong, C., Wang, Y., Steel, R.J., Olariu, C., Xu, Q., Liu, X., Zhao, Q., 2015b. Growth Styles of Shelf-Margin Clinoforms: Prediction of Sand- and Sediment-Budget Partitioning Into and Across The Shelf. Journal of Sedimentary Research 85, 209–229.

Helland-Hansen, W., Sømme, T.O., Martinsen, O.J., Lunt, I., Thurmond, J., 2016. Deciphering Earth's Natural Hourglasses: Perspectives On Source-To-Sink Analysis. Journal of Sedimentary Research 86, 1008–1033.

Henriksen, S., Helland-Hansen, W., Bullimore, S., 2011. Relationships between shelf-edge trajectories and sediment dispersal along depositional dip and strike: A different approach to sequence stratigraphy. Basin Research 23, 3–21.

Kempton, R.H., Bourdet, J., Gong, S., Ross, A.S., 2020. Revealing oil migration in the frontier Bight Basin, Australia. Marine and Petroleum Geology 113.

Krassay, A.A., Totterdell, J.M., 2003. Seismic stratigraphy of a large, Cretaceous shelf-margin delta complex, offshore southern Australia. AAPG Bulletin 87, 935–963.

MacDonald, J.D., Holford, S.P., Green, P.F., Duddy, I.R., King, R.C., Backé, G., 2013. Detrital zircon data reveal the origin of Australia's largest delta system. Journal of the Geological Society 170, 3–6.

Mitchum, R.M., Vail, P.R., Thompson, S., 1977. Seismic Stratigraphy and Global Changes of Sea Level. Part 2. The Depositional Sequence as a Basic Unit for Stratigraphic Analysis: Section 2. Application of Seismic Reflection Configuration to Stratigraphic Interpretation, in: Payton, C.E. (Ed.), Seismic Stratigraphy: Applications to Hydrocarbon Exploration. American Association of Petroleum Geologists, pp. 53–62.

Morgan, R.P., 2014. Infilled Palynology of Gnarlyknots-1A, Bight Basin, South Australia.

Patruno, S., Hampson, G.J., Jackson, C.A.L., 2015. Quantitative characterisation of deltaic and subaqueous clinoforms. Earth-Science Reviews 142, 79–119.

Paumard, V., Bourget, J., Durot, B., Lacaze, S., Payenberg, T., George, A.D., Lang, S., 2019a. Full-volume 3D seismic interpretation methods: A new step towards high-resolution seismic stratigraphy. Interpretation 7, B33–B47.

Paumard, V., Bourget, J., Payenberg, T., George, A.D., Ainsworth, R.B., Lang, S., 2019b. From quantitative 3D seismic stratigraphy to sequence stratigraphy: Insights into the vertical and lateral variability of shelf-margin depositional systems at different stratigraphic orders. Marine and Petroleum Geology 110, 797–831.

Paumard, V., Bourget, J., Payenberg, T., George, A.D., Bruce Ainsworth, R., Lang, S., Posamentier, H.W., 2020. Controls on deep-water sand delivery beyond the shelf edge: Accommodation, sediment supply, and deltaic process regime. Journal of Sedimentary Research 90, 104–130.

Pellegrini, C., Patruno, S., Helland-Hansen, W., Steel, R.J., Trincardi, F., 2020. Clinoforms and clinothems: Fundamental elements of basin infill. Basin Research 32, 187–205.

Totterdell, J.M., Blevin, J.E., Struckmeyer, H.I.M., Bradshaw, B.E., Colwell, J.B., Kennard, J.M., 2000. A new sequence framework for the Great Australia Bight: Starting with a clean slate. The Appea Journal 40, 95–118.

Vail, P.R., Audemart, F., Bowman, S.A., Eisner, P.N., Perez-Cruz, G., 1991. The stratigraphic signatures of tectonics, eustasy and sedimentation—an overview, in: Einsele, G. (Ed.), Cycles and Events in Stratigraphy. Springer Verlag, New York, pp. 617–659.

Vail, P.R., Mitchum, R.M., Thompson, S., 1977. Seismic stratigraphy and global changes of sea level. Part 3: relative changes of sea level from coastal onlap, in: Payton, C.E. (Ed.), Seismic Stratigraphy - Applications to Hydrocarbon Exploration: American Association of Petroleum Geologists. American Association of Petroleum Geologists, pp. 63–81.

Whiteway, T., 2009. Australian bathymetry and topography grid, June 2009.